Regulation of the tubulin polymerization-promoting protein by Ca^{2+}/S100 proteins

Seita Doi[a], Naoki Fujioka[b], Satomi Ohtsuka[a], Rina Kondo[a], Maho Yamamoto[a], Miwako Denda[c], Masaki Magari[a], Naoki Kanayama[a], Naoya Hatano[a], Ryo Morishita[c], Takafumi Hasegawa[d], and Hiroshi Tokumitsu[a,*]

[a]Applied Cell Biology, Graduate School of Interdisciplinary Science and Engineering in Health Systems, Okayama University, Okayama 700-8530 Japan

[b]Department of Applied Chemistry and Biotechnology, Faculty of Engineering, Okayama University, Okayama 700-8530, Japan

[c]CellFree Sciences Co., Ltd, Matsuyama, 790-8577, Japan

[d]Division of Neurology, Department of Neuroscience and Sensory Organs, Tohoku University Graduate School of Medicine, Sendai, 980-8574, Japan

**To whom correspondence should be addressed: Hiroshi Tokumitsu, Ph.D.
Applied Cell Biology, Graduate School of Interdisciplinary Science and Engineering in Health Systems, Okayama University, 3-1-1 Tsushima-naka, Kita-ku, Okayama 700-8530, Japan.
Tel/FAX: +81-86-251-8197; E-mail: tokumit@okayama-u.ac.jp

Running title: *TPPP as a novel S100 protein target*

Conflict of Interest: The authors declare that they have no conflicts of interest with the contents of this article.

The abbreviations used are: ARG2, arginase-2 mitochondrial precursor; CDR2L, cerebellar degeneration-related protein 2-like; DTNBP1, dystrobrevin-binding protein 1; MED29, mediator complex subunit 29; MRPS34, mitochondrial ribosomal protein S34; OIP5, Opa interacting protein 5; RPL36, 60S ribosomal protein L36; SNRPB2, small nuclear ribonucleoprotein polypeptide B"; TMLHE, trimethyllysine dioxygenase, mitochondrial isoform 1 precursor; TPPP, tubulin polymerization-promoting protein; TRH, thyrotropin-releasing hormone preproprotein; PPI, protein–protein interaction; NHS, N-hydroxysuccinimide; EDC, 1-ethyl-3-(3-dimethylaminopropyl) carbodiimide hydrochloride

Author contributions: Seita Doi: Visualization, Investigation, Writing-Reviewing and Editing. **Naoki Fujioka:** Visualization, Investigation. **Satomi Ohtsuka:** Investigation for revised manuscript. **Rina Kondo:** Investigation, Data curation. **Maho Yamamoto:** Investigation, Data curation. **Miwako Denda:** Investigation, Data curation. **Masaki Magari*:*** Supervision. **Naoki Kanayama*:*** Supervision, Writing-Reviewing and Editing. **Naoya Hatano:** Writing- Reviewing and Editing. **Ryo Morishita:** Methodology, Writing-Reviewing and Editing. **Takafumi Hasegawa:** Resources, Writing-Reviewing and Editing. **Hiroshi Tokumitsu:** Conceptualization, Writing-Original Draft, Writing-Reviewing and Editing.

Abstract

To elucidate S100 protein-mediated signaling pathways, we attempted to identify novel binding partners for S100A2 by screening protein arrays carrying 19,676 recombinant glutathione S-transferase (GST)-fused human proteins with biotinylated S100A2. Among newly discovered putative S100A2 interactants, including TMLHE, TRH, RPL36, MRPS34, CDR2L, OIP5, and MED29, we identified and characterized the tubulin polymerization-promoting protein (TPPP) as a novel S100A2-binding protein. We confirmed the interaction of TPPP with Ca^{2+}/S100A2 by multiple independent methods, including the protein array method, S100A2 overlay, and pulldown assay *in vitro* and in transfected COS-7 cells. Based on the results from the S100A2 overlay assay using various GST-TPPP mutants, the S100A2-binding region was identified in the C-terminal (residues 111–160) of the central core domain of a monomeric form of TPPP that is involved in TPPP dimerization. Chemical cross-linking experiments indicated that S100A2 suppresses dimer formation of His-tagged TPPP in a dose-dependent and a Ca^{2+}-dependent manner. In addition to S100A2, TPPP dimerization is disrupted by other multiple S100 proteins, including S100A6 and S100B, in a Ca^{2+}-dependent manner but not by S100A4. This is consistent with the fact that S100A6 and S100B, but not S100A4, are capable of interacting with GST-TPPP in the presence of Ca^{2+}. Considering these results together, TPPP was identified as a novel target for S100A2, and it is a potential binding target for other multiple S100 proteins, including S100A6 and S100B. Direct binding of the S100 proteins with TPPP may cause disassembly of TPPP dimer formation in response

61 to the increasing concentration of intracellular Ca^{2+}, thus resulting in the regulation of the

62 physiological function of TPPP, such as microtubule organization.

63

Introduction

S100 proteins constitute two classes of the EF hand-type Ca^{2+}-binding protein family, which is involved in various intracellular Ca^{2+} signaling and extracellular activities via secretions of family members such as S100B, S100A8, and S100A9 [1-3]. Accumulated evidence indicates that S100 proteins are differentially expressed in a wide variety of cell types that interact with specific or redundant target proteins to transduce intracellular or extracellular signaling. Ca^{2+} binding induces conformational changes of S100 proteins, which results in exposure of a hydrophobic cleft that is essential for S100/targets interaction [4]. Unlike the major Ca^{2+} mediator, calmodulin, whose target interactions are classified as 1–10, 1–14, 1–16, and IQ motifs [5], S100 proteins interact with their interactants through various binding motifs, as was revealed through crystal structure analysis [6]. The tetratricopeptide repeat motif in cyclophilin 40, FKBP52, CHIP (C terminus of Hsc70-interacting protein), FKBP38, and protein phosphatase 5 was shown to interact with S100 proteins, including S100A1, S100A2, S100A6, and S100B [7-10]. Although the molecular mechanism(s) have not been elucidated, conflicting results about the role of S100A2 in tumor suppression [11] and cancer metastasis [12, 13] have been published. In intact cells, S100A2 is localized in the cytoplasm and nucleus [14] and is secreted in extracellular space. In the cytoplasm, S100A2 interacts with various proteins, including enzymes [10] and cytoskeletal proteins [15]. Additionally, S100A2 interacts with monomeric and tetrameric forms of the tumor suppressor p53 [16], which modulates its transcriptional activity [17], and with the receptor for advanced glycation end-products [18]. To investigate the multifunctional roles of S100A2, we set up genome-wide protein–protein interaction

(PPI) screening using human protein arrays containing 19,676 recombinant human proteins to identify potential S100A2 target proteins. By screening the human protein arrays with biotinylated calmodulin and S100A6, the striated muscle activator of Rho signaling [19] and FOR20 were identified as novel calmodulin- and S100A6-binding proteins [20], respectively, which indicates that genome-wide PPI screening is an effective and time-saving method for comprehensive identification of potential interactants for various Ca^{2+} mediators. In this report, we identified multiple candidates for S100A2 target proteins through comprehensive PPI screening and characterized TPPP/p25 (tubulin polymerization-promoting protein) as a novel S100A2 target that may be a target for multiple S100 proteins. According to our biochemical characterization of TPPP/S100 protein interaction, we demonstrated for the first time the Ca^{2+}-dependent regulation of TPPP dimerization via direct interaction with S100 proteins.

2. Materials and Methods

***2.1. Materials*---**S100 proteins (S100A2, S100A4, S100A6, and S100B) were expressed in *Escherichia coli* (*E. coli*) BL21 (DE3) using the pET vector and were purified by Phenyl-Sepharose chromatography following a previously described method (see Supplemental Figure S1) [20]. Recombinant S100A2 was biotinylated with biotinoyl-ε-aminocaproic acid N-hydroxysuccinimide (NHS) ester followed by purification [21]. Human TPPP cDNA (NM_007030.3) was cloned and subcloned into pcDNA3.1+ (Invitrogen, CA, USA) as HA-tagged cDNA [22]. Anti-glutathione S-transferase (GST) and anti-His tag antibodies were obtained from GE Healthcare UK, Ltd. (Buckinghamshire, UK) and Proteintech

(Rosemont, IL, USA), respectively. Anti-S100A2 antibody was obtained from R&D Systems (Minneapolis, MN, USA). All other chemicals were obtained from standard commercial sources.

***2.2. Screening of S100A2 targets using human protein array*---**Protein array plates (Protein Active Array®, 1,536-well format × 27 plates) containing 19,676 recombinant human proteins in duplicate generated by wheat germ cell-free protein synthesis were constructed by CellFree Sciences (Matsuyama, Japan) [19], and the PPI screening was performed by incubation with 0.6 μg/mL biotinylated S100A2 in the presence of 1 mM $CaCl_2$, followed by a streptavidin–horseradish peroxidase-mediated enhanced chemiluminescence (ECL) detection of S100A2 binding with ChemiDoc™ XRS (Bio-Rad Laboratories, Hercules, CA, USA) [20].

2.3. Expression of GST-fused proteins by wheat germ cell-free protein synthesis*---**Potential targets of S100A2 interactants (TMLHE, NP_060666; TPPP, NP_008961; TRH, NP_009048; DTNBP1, NP_115498; ARG2, NP_001163; RPL36, NP_056229; MRPS34, NP_076425; SNRPB2, NP_003083; CDR2L, NP_055418; OIP5, NP_009211; and MED29, NP_060062) were identified by protein assay screening as described in ***2.2 (see Fig. 1), were generated by wheat germ cell-free protein synthesis using the WEPRO7240G Expression Kit (CellFree Sciences) as GST-fusion proteins [19, 23], and then were subsequently analyzed via S100A2 overlay and immunoblotting using an anti-GST antibody.

***2.4. Construction, expression, and purification of GST-TPPP-His$_6$ and TPPP-His$_6$*---**Human TPPP cDNA was amplified by polymerase chain reaction (PCR) using PrimeSTAR HS DNA polymerase (Takara Bio, Shiga, Japan) and pcDNA3.1-HA-TPPP, as described above, as a template with a sense primer (5′-gggtctagacgctgacaaggcc-3′) and an antisense primer (5′-cttgccccttgcaccttctgg-3′) for

pGEX-PreS-His_6 vector. The cDNA was then subcloned into the pGEX-PreS-His_6 vector (*XbaI/SmaI* site; [24]), which resulted in pGEX-PreS-TPPP wild-type (2–219)-His_6. Truncation and deletion mutants of GST-TPPP-His_6 were constructed by PCR using PrimeSTAR HS DNA polymerase using the following primer pairs:

GST-TPPP (2–174)-His_6: 5′-gggtctagacgctgacaaggcc-3′/5′-ggagcccgtgaacttggtggt-3′

GST-TPPP (2–100)-His_6: 5′-gggtctagacgctgacaaggcc-3′/5′-gctgaagacgatgtccacgtcagtg-3′

GST-TPPP (101–174)-His_6: 5′-gggtctagacaagatcaaagggaagtcttg-3′/5′-ggagcccgtgaacttggtggt-3′

GST-TPPP (120–174)-His_6: 5′-gggtctagacgaggagctcgc-3′/5′-ggagcccgtgaacttggtggt-3′

GST-TPPP (111–160)-His_6: 5′-gggtctagacacctttgagcagttcc-3′/5′- gggcgacgagatggcttt-3′

GST-TPPP (111–150)-His_6: 5′- gggtctagacacctttgagcagttcc-3′/5′- gatgatgggcgccttgccct-3′

Mammalian expression plasmids for GST-TPPP was constructed by PCR using primer pairs (5′-gccaccatgtcccctatactaggttattgg-3′/5'-gggctcgagctacttgcccc-3') and a template DNA (pGEX-PreS-TPPP wild-type) as described above, followed by subcloning into the pME18s vector. The nucleotide sequences of all constructs were confirmed by sequencing using an ABI PRISM 310 Genetic Analyzer (Applied Biosystems, Foster City, CA, USA). Recombinant GST-TPPP-His_6 proteins, including various mutants, were expressed in *E. coli* BL21(DE3) and were purified by glutathione-Sepharose chromatography, followed by Ni-Sepharose chromatography (GE Healthcare UK), as described in the manufacturer's protocol. TPPP-His_6 was obtained by the digestion of GST-TPPP-His_6 with PreScission Protease (GE Healthcare UK) to remove GST, followed by purification with Ni-Sepharose

chromatography. Mammalian expression plasmids for GST-TPPP were constructed using the pME18s vector.

2.5. S100 proteins/TPPP interaction assay---Purified GST-TPPP-His_6 (40 μg) or TPPP-His_6 (20 μg) was incubated with S100 proteins (20 μg for TPPP-His_6 and 40 μg for GST-TPPP-His_6) in a solution (500 μL) containing 150 mM NaCl, 20 mM Tris-HCl (pH 7.5), and 0.05% Tween 20 (+30 mM imidazole for TPPP-His_6 pulldown) in the absence (for TPPP-His_6 pulldown) or presence of 2 mM $CaCl_2$ or 2 mM ethylene glycol-bis(β-aminoethyl ether)-N,N,N′,N′-tetraacetic acid (EGTA) for 1 h at 4℃. Subsequently, 50 μL of either glutathione-Sepharose or Ni-Sepharose beads (50% slurry, GE Healthcare UK, Ltd.) were incubated with the sample followed by incubation for 1 h. After extensive washing, 1× sodium dodecyl sulfate–polyacrylamide gel electrophoresis (SDS-PAGE) sample buffer (for GST-TPPP-His_6) (50 μL) or an elution buffer containing-300 mM imidazole (50 μL) was added to the beads. Samples (10 μL) were analyzed on a Tris-Tricine-SDS-10% polyacrylamide gel using Coomassie Brilliant Blue (CBB) staining or immunoblot analysis.

2.6. Cell culture, transfection and GST precipitation assay---COS-7 cells were cultured in Dulbecco's modified Eagle's medium supplemented with 10% fetal bovine serum (FBS), 100 U/mL penicillin, and 100 U/mL streptomycin at 37°C in 5% CO_2. Cultured COS-7 cells were plated on 10-cm dishes and transfected with 2 μg of GST-TPPP expression plasmid (pME-GST-TPPP) and 8 μg of S100A2 expression plasmid (pME-S100A2 [7]) using polyethyleneimine "MAX" (Polysciences, Inc., Warrington, PA), in accordance with the manufacturer's protocol. After 48 h of culture, the cells were lysed with 1 mL of ice-cold lysis buffer (150 mM NaCl, 20 mM Tris-HCl, pH 7.5, 0.05% Tween20, 0.2

163 mM PMSF, and either 2 mM EGTA or 2 mM $CaCl_2$) and centrifuged at 17,970 × *g* for 10 min to obtain
164 the cell lysate. The GST precipitation assay was then performed as described above, followed by
165 immunoblot analysis using antibodies to GST and S100A2.

166 ***2.7. TPPP dimerization assay***---Recombinant TPPP-His_6 (2.0 μg) was incubated with or without S100
167 proteins (0.5–1.5 μg) in a solution (40 μL) containing 90 mM NHS/39 mM 1-ethyl-3-(3-
168 dimethylaminopropyl) carbodiimide hydrochloride (EDC) in the presence or absence of 2 mM $CaCl_2$
169 for 1 h at 25°C. The cross-linking reaction was terminated by the addition of 2-mercaptoethanol
170 (10 M) and was subjected to SDS-PAGE, followed by CBB staining or immunoblot analysis using the
171 anti-His tag antibody.

172 ***2.8. Other methods*---**Immunoblot analysis was conducted using the indicated primary antibodies
173 with horseradish peroxidase-conjugated anti-mouse, anti-rabbit IgG (GE Healthcare UK,
174 Buckinghamshire, UK), or anti-goat IgG (Southern Biotech, Birmingham, AL, USA) as the secondary
175 antibody. An ECL reagent (Perkin Elmer, Waltham, MA, USA) was used for signal detection. The
176 S100A2 overlay method, using biotinylated S100A2 (0.6 μg/mL) in the presence of either 2 mM $CaCl_2$
177 or 2 mM EGTA, was performed as previously described [21]. Dot blot analysis of biotinylated S100A2
178 was conducted using streptavidin–horseradish peroxidase conjugate (GE Healthcare UK, Ltd.,
179 Buckinghamshire, UK) and the ECL detection system as described above. The protein concentration
180 was estimated by staining with CBB (Bio-Rad Laboratories, Inc., Hercules, CA), using bovine serum
181 albumin as the standard.

182

3. Results

***3.1. Protein array screening of S100A2-binding proteins*---**To identify S100A2 targets comprehensively, we performed a PPI assay using Protein Active Array® (CellFree Sciences, Matsuyama, Japan) containing 19,676 recombinant human proteins as GST-fused proteins generated by wheat germ cell-free protein synthesis [19] for interaction with biotinylated S100A2 as a protein ligand (Fig. 1). Purified biotinylated S100A2 (Fig. 1A, *left panel*) was readily detected at 1 ng using the avidin–HRP-mediated detection system (Fig. 1A, *right panel*). PPI screening of 19,676 human proteins with biotinylated S100A2 (0.6 μg/mL) in the presence of 1 mM $CaCl_2$ revealed several positive S100A2-binding signals, including trimethyllysine dioxygenase, mitochondrial isoform 1 precursor (TMLHE) [25], TPPP/P25 [26], thyrotropin-releasing hormone preproprotein (TRH) [27], dystrobrevin-binding protein 1 (DTNBP1) [28], arginase-2 mitochondrial precursor (ARG2) [29], 60S ribosomal protein L36 (RPL36) [30], mitochondrial ribosomal protein S34 (MRPS34) [31], small nuclear ribonucleoprotein polypeptide B" (SNRPB2) [32], cerebellar degeneration-related protein 2-like (CDR2L) [33], Opa interacting protein 5 (OIP5) [34], and mediator complex subunit 29 (MED29) [35](Fig. 1B). To confirm the S100A2-binding ability of newly identified S100A2 targets, we performed a biotinylated S100A2 overlay against the proteins generated by the wheat germ cell-free protein synthesis as GST-fusion proteins, including the Venus protein (Venus) and an empty vector (Mock) as the negative controls. Immunoblot analysis using an anti-GST antibody indicated the comparable synthesis level of all candidates for S100A2 interactants (Fig. 1C, *upper panel*). Among 11 candidate proteins as S100A2 targets, eight proteins (TMLHE, TPPP, TRH, RPL36,

MRPS34, CDR2L, OIP5, and MED29) were capable of binding to S100A2, but three proteins (DTNBP1, ARG2, and SNRPB2) were not (Fig. 1C, *lower panel*). These results suggest that TMLHE, TPPP, TRH, RPL36, MRPS34, CDR2L, OIP5, and MED29 contain putative S100A2-binding regions that are functional under denatured conditions on SDS-PAGE and that DTNBP1, ARG2, and SNRPB2 may require native conformation for S100A2 binding.

***3.2. S100 protein binding to TPPP in vitro and in transfected COS-7 cells*---**We chose to further characterize TPPP as a novel S100A2-binding protein and the characterization of other potential S100A2 interactants will be described in detail in subsequent studies. TPPP interacts with tubulin and microtubules, which results in microtubules bundling through the dimerization property [36, 37]. However, the regulatory mechanism of the TPPP function including dimerization-mediated microtubules bundling is not clear. First, we examined the S100 protein/TPPP interaction under the native condition by the pulldown assay using purified His-tagged TPPP (TPPP-His_6) and S100A2 (Fig. 2A). Recombinant S100A2 was incubated together with or without TPPP-His_6 in either the presence or absence of 2 mM $CaCl_2$, followed by pulldown with Ni-Sepharose resin. We confirmed that S100A2 interacted with TPPP-His_6 in a Ca^{2+}-dependent manner *in vitro* without non-specific binding with Ni-Sepharose resin (Fig. 2A). We next examined whether the S100A2–TPPP interaction occurs in intact cells. COS-7 cells were transfected with expression plasmids encoding GST-TPPP and S100A2. GST-TPPP protein was then pulled down with glutathione-Sepharose in the absence or presence of Ca^{2+} (Fig. 2B, *third panel*). Immunoblot analysis of the precipitated samples with an anti-S100A2 antibody revealed that S100A2 exogenously expressed in COS-7 cells was co-precipitated

with GST-TPPP only in the presence of 2 mM $CaCl_2$ (Fig. 2B, *bottom panel*). To examine the specificity of S100 proteins for TPPP binding, we checked four S100 proteins (S100A2, S100A4, S100A6, and S100B) for TPPP interaction by using the pulldown experiment with GST-TPPP-His_6. Consistent with Fig. 2A, S100A2 has been shown to interact with GST-TPPP-His_6 in a Ca^{2+}-dependent manner (Fig. 2B) without non-specific binding with glutathione-Sepharose resin (Supplemental Figure S2). In addition to S100A2, S100A6 and S100B are capable of Ca^{2+}-dependent interaction with GST-TPPP-His_6, but not S100A4, which indicates that S100/TPPP interaction can occur in various cell types and tissues, since the expression of S100 proteins varied in a tissue- and cell-type-specific manner.

***3.3. Mapping of the S100A2-binding region on TPPP*---**Next, we attempted to map the S100A2-binding region on TPPP by using the biotinylated S100A2 overlay method against various GST-TPPP-His_6 mutants, including the full-length protein (Fig. 3A). GST-fused TPPP-His_6 proteins were purified by glutathione-Sepharose chromatography and subjected to immunoblot analysis using the anti-His tag antibody to measure the amounts of proteins loaded on the SDS-PAGE and S100A2 overlay to evaluate S100A2-binding ability (Fig. 3B, *right panel*). Consistent with the result for GST-TPPP generated by the wheat germ cell-free protein synthesis, as shown in Fig. 1C, full-length GST-TPPP (residues 2–219)-His_6 and the C-terminal truncated mutant (residues 2–174) lacking a C-terminal unstructured domain (residues 175-219) were capable of binding with S100A2 (Fig. 3B, *left panel*). A C-terminal truncation mutant (residues 2–100) lacking the C-terminal 74 residues of the central core domain impaired S100A2-binding ability, which is consistent with that of the TPPP mutants-

243 containing residues 101–174 and residues 111–160 in the core domain maintaining S100A2-binding
244 ability. Mutants-containing residues 120–174 and residues 111–150 were incapable of binding with
245 S100A2, which indicates that S100A2 binds to a monomeric TPPP, and a putative S100A2-binding
246 site is located in the C-terminal half region (residues 111–160) of the TPPP core domain.

247 ***3.4. Effect of S100A2 on TPPP dimerization activity*---**TPPP forms dimers through its central core
248 domain, which is involved in microtubule bundling [37], which results in the regulation of mitotic
249 spindle formation [38]. Therefore, we used the zero-length chemical cross-linking method with
250 NHS/EDC to test whether S100A2 affects TPPP dimerization (Fig. 4). We successfully detected cross-
251 linked dimer formation of purified TPPP-His_6 (~60 kDa on SDS-PAGE) and monomeric TPPP (~30 kDa
252 on SDS-PAGE) (Figs. 4A and B). We added various concentrations of S100A2 to TPPP-His_6 prior to a
253 cross-linking reaction were initiated with NHS/EDC, which was observed with SDS-PAGE analysis (Fig.
254 4A). CBB staining of SDS-PAGE gel revealed that the amount of the TPPP-His_6 dimer at ~60 kDa
255 gradually decreased as the concentration of S100A2 increased in the presence of 2 mM $CaCl_2$, but a
256 higher molecular mass was not observed in the TPPP-His_6 dimer complexed with S100A2. Instead,
257 the amounts of TPPP-His_6 monomer cross-linked with S100A2 dimer (~45 kDa, Fig. 4B *asterisk*) and
258 monomer (~35 kDa, Fig. 4B) increased. The effect of S100A2 on TPPP-His_6 dimerization via chemical
259 cross-linking was assayed in the presence or absence of 2 mM $CaCl_2$ by immunoblot analysis using
260 the anti-His tag antibody (Fig. 4B). Consistent with Fig. 4A, TPPP dimer formation was disassembled
261 because of the addition of S100A2 in the presence of $CaCl_2$ but not in the absence of $CaCl_2$, which

indicated that the TPPP dimerization activity was controlled by direct S100A2 binding in a Ca^{2+}-dependent manner (Fig. 4C).

***3.5. Effect of S100 protein family on TPPP dimerization activity*---**Since TPPP colocalizes with S100 in oligodendroglia-like cells [39] and S100B is highly expressed in oligodendrocytes among the S100 protein family [40, 41], we tested the effect of various S100 family proteins, including S100B on TPPP-His_6 dimerization, which were tested for their ability to bind to TPPP (Fig. 2B). S100A4 did not suppress TPPP-His_6 dimerization, regardless of the presence or absence of Ca^{2+} (Fig. 5A), which was consistent with the fact that S100A4 is unable to bind GST-TPPP-His_6 (Fig. 2B). S100A6 (Fig. 5B) and S100B (Fig. 5C) interact with the TPPP-His_6 monomer with molecular masses of ~45 kDa (S100 dimer:TPPP-His_6 monomer complex, *asterisks*) and ~35 kDa (S100 monomer:TPPP-His_6 monomer complex), which result in effectively disassembling TPPP dimerization in a dose-dependent and Ca^{2+}-dependent manner, which was similar to S100A2 (Fig. 4). Cross-linked products of monomeric forms of S100 proteins with TPPP-His_6 with a molecular mass of ~35 kDa (Fig. 4, Fig. 5B, and Fig. 5C) were observed, probably due to incomplete chemical cross-linking of S100 dimeric complex.

4. Discussion

Ca^{2+} signaling regulates a wide variety of physiological responses, including cytoskeletal organization, muscle contraction, neuronal, metabolic, and pathophysiological pathways through various Ca^{2+} mediators, including calmodulin, S100 proteins, and other Ca^{2+} receptors [42]. In contrast to calmodulin, which regulates various enzymes, such as protein kinases (CaM-kinases), phosphatase

282 (calcineurin), nitric oxide synthase, cyclic nucleotide phosphodiesterase, and adenylate cyclase in a
283 Ca^{2+}-dependent manner [43], the S100 protein family is composed of more than 20 members of
284 isoproteins and highly conserved in mice and humans [3, 44]; however, the contribution of S100
285 proteins to the Ca^{2+}-dependent physiological intracellular process is still not fully understood.
286 Therefore, we tried to identify a physiologically relevant target(s) for S100 proteins by using
287 genome-wide comprehensive PPI assay [20]. In this report, we screened human protein arrays with
288 biotinylated S100A2 and identified 11 novel putative S100A2-binding proteins (Fig. 1). Among them,
289 we chose the TPPP/p25 for further biochemical characterization of the interaction with S100
290 proteins. Based on its interaction with S100 proteins, TPPP/p25 is a potential target protein for
291 multiple S100 proteins, including S100A6 and S100B. Furthermore, TPPP/p25 was identified as a
292 brain-specific [45] and a novel microtubule-associated protein that is capable of inducing the
293 polymerization of tubulin [36], which results in the reorganization of a microtubule network. TPPP
294 forms a dimer through its flexible core domain, which is important for microtubule-bundling activity,
295 since the unstructured N- and C-terminal domains interact with other microtubules, thus resulting
296 in their cross-linking [46]. Here we discovered that S100 proteins, including S100A2, S100A6, and
297 S100B, are capable of suppressing TPPP dimerization activity in a Ca^{2+}-dependent manner *in vitro*.
298 Ca^{2+}-dependent S100A2–TPPP interaction was also confirmed in transfected cultured cells (Fig. 2B).
299 The S100 proteins interact with TPPP, whose S100A2-binding region is mapped in the flexible central
300 core domain (Fig. 3), thus suggesting that the S100 proteins block TPPP dimerization through the
301 steric hindrance due to their Ca^{2+}-dependent direct interaction with TPPP (Fig. 4C). Thus, TPPP is

highly enriched in oligodendrocytes and S100B [39], which suggests that S100B is a *bona fide* regulator controlling TPPP-mediated microtubule organization, which could depend on the concentration of intracellular Ca^{2+} in oligodendrocytes. Recently, Fu *et al* reported that TPPP on Golgi outposts is involved in local microtubule nucleation and myelin sheath elongation [47]. These physiological functions of TPPP might be regulated by Ca^{2+}/S100 proteins. Interestingly, S100B is associated with microtubular structures in oligodendrocytes, which suggests that it has a regulatory function for cell morphology and cytoskeletal organization [48]. It has been shown that S100B inhibits the polymerization of purified tubulin as well as purified microtubule protein, resulting in microtubule disassembly *in vitro [49-51]*. In astrocytes (U251 glioma cells) which apparently do not express TPPP, S100B has demonstrated to cause microtubule disassembly by interacting with the microtubules [52]. These results may suggest that S100B regulates microtubule assembly either directly or indirectly through S100B-target protein such as TPPP, that could be depending on cell-types. In pathological conditions, TPPP/p25 is enriched in filamentous α-synuclein-bearing Lewy bodies of Parkinson's disease as well as glial cytoplasmic inclusions of multiple system atrophy [53], which is consistent with a finding of TPPP-induced oligomerization of α-synuclein [22]. TPPP interacts with α-synuclein through the C-terminal of the core domain (residues 147–156) [54], which could overlap the S100 protein-binding region (residues 111–160), thus suggesting the possible involvement of Ca^{2+}/S100 proteins in the given pathological condition. Therefore, we will test our hypothesis to determine whether S100 proteins regulate the TPPP function *in vivo* in a Ca^{2+}-

dependent manner, including dimerization-mediated microtubule organization and α-synuclein aggregation, in a subsequent study.

5. References

[1] R. Donato, S100: a multigenic family of calcium-modulated proteins of the EF-hand type with intracellular and extracellular functional roles, Int J Biochem Cell Biol, 33 (2001) 637-668.

[2] C.W. Heizmann, G. Fritz, B.W. Schafer, S100 proteins: structure, functions and pathology, Front Biosci, 7 (2002) d1356-1368.

[3] R. Donato, B.R. Cannon, G. Sorci, F. Riuzzi, K. Hsu, D.J. Weber, C.L. Geczy, Functions of S100 proteins, Curr Mol Med, 13 (2013) 24-57.

[4] S. Bhattacharya, C.G. Bunick, W.J. Chazin, Target selectivity in EF-hand calcium binding proteins, Biochim Biophys Acta, 1742 (2004) 69-79.

[5] K.L. Yap, J. Kim, K. Truong, M. Sherman, T. Yuan, M. Ikura, Calmodulin target database, J Struct Funct Genomics, 1 (2000) 8-14.

[6] B. Kiss, P. Ecsedi, M. Simon, L. Nyitray, Isolation and Characterization of S100 Protein-Protein Complexes, Methods Mol Biol, 1929 (2019) 325-338.

[7] S. Shimamoto, Y. Kubota, H. Tokumitsu, R. Kobayashi, S100 proteins regulate the interaction of Hsp90 with Cyclophilin 40 and FKBP52 through their tetratricopeptide repeats, FEBS Lett, 584 (2010) 1119-1125.

[8] S. Shimamoto, Y. Kubota, F. Yamaguchi, H. Tokumitsu, R. Kobayashi, Ca^{2+}/S100 proteins act as

upstream regulators of the chaperone-associated ubiquitin ligase CHIP (C terminus of Hsc70-interacting protein), J Biol Chem, 288 (2013) 7158-7168.

[9] S. Shimamoto, M. Tsuchiya, F. Yamaguchi, Y. Kubota, H. Tokumitsu, R. Kobayashi, Ca^{2+}/S100 proteins inhibit the interaction of FKBP38 with Bcl-2 and Hsp90, Biochem J, 458 (2014) 141-152.

[10] F. Yamaguchi, Y. Umeda, S. Shimamoto, M. Tsuchiya, H. Tokumitsu, M. Tokuda, R. Kobayashi, S100 proteins modulate protein phosphatase 5 function: a link between Ca^{2+} signal transduction and protein dephosphorylation, J Biol Chem, 287 (2012) 13787-13798.

[11] G. Feng, X. Xu, E.M. Youssef, R. Lotan, Diminished expression of S100A2, a putative tumor suppressor, at early stage of human lung carcinogenesis, Cancer Res, 61 (2001) 7999-8004.

[12] E. Bulk, B. Sargin, U. Krug, A. Hascher, Y. Jun, M. Knop, C. Kerkhoff, V. Gerke, R. Liersch, R.M. Mesters, M. Hotfilder, A. Marra, S. Koschmieder, M. Dugas, W.E. Berdel, H. Serve, C. Muller-Tidow, S100A2 induces metastasis in non-small cell lung cancer, Clin Cancer Res, 15 (2009) 22-29.

[13] A. Naba, K.R. Clauser, J.M. Lamar, S.A. Carr, R.O. Hynes, Extracellular matrix signatures of human mammary carcinoma identify novel metastasis promoters, Elife, 3 (2014) e01308.

[14] R. Deshpande, T.L. Woods, J. Fu, T. Zhang, S.W. Stoll, J.T. Elder, Biochemical characterization of S100A2 in human keratinocytes: subcellular localization, dimerization, and oxidative cross-linking, J Invest Dermatol, 115 (2000) 477-485.

[15] M. Gimona, Z. Lando, Y. Dolginov, J. Vandekerckhove, R. Kobayashi, A. Sobieszek, D.M. Helfman, Ca^{2+}-dependent interaction of S100A2 with muscle and nonmuscle tropomyosins, J Cell Sci, 110 (Pt 5) (1997) 611-621.

[16] J. van Dieck, M.R. Fernandez-Fernandez, D.B. Veprintsev, A.R. Fersht, Modulation of the oligomerization state of p53 by differential binding of proteins of the S100 family to p53 monomers and tetramers, J Biol Chem, 284 (2009) 13804-13811.

[17] A. Mueller, B.W. Schafer, S. Ferrari, M. Weibel, M. Makek, M. Hochli, C.W. Heizmann, The calcium-binding protein S100A2 interacts with p53 and modulates its transcriptional activity, J Biol Chem, 280 (2005) 29186-29193.

[18] E. Leclerc, G. Fritz, S.W. Vetter, C.W. Heizmann, Binding of S100 proteins to RAGE: an update, Biochim Biophys Acta, 1793 (2009) 993-1007.

[19] Y. Furuya, M. Denda, K. Sakane, T. Ogusu, S. Takahashi, M. Magari, N. Kanayama, R. Morishita, H. Tokumitsu, Identification of striated muscle activator of Rho signaling (STARS) as a novel calmodulin target by a newly developed genome-wide screen, Cell Calcium, 60 (2016) 32-40.

[20] K. Sakane, M. Nishiguchi, M. Denda, F. Yamagchi, M. Magari, N. Kanayama, R. Morishita, H. Tokumitsu, Identification and characterization of a centrosomal protein, FOR20 as a novel S100A6 target, Biochem Biophys Res Commun, 491 (2017) 980-985.

[21] K. Sakane, F. Yamaguchi, M. Tsuchiya, R. Kondo, N. Kanayama, M. Magari, N. Hatano, R. Kobayashi, H. Tokumitsu, Interaction of S100A6 with Target Proteins In Vitro and in Living Cells, Methods Mol Biol, 1929 (2019) 367-377.

[22] T. Hasegawa, T. Baba, M. Kobayashi, M. Konno, N. Sugeno, A. Kikuchi, Y. Itoyama, A. Takeda, Role of TPPP/p25 on alpha-synuclein-mediated oligodendroglial degeneration and the protective effect of SIRT2 inhibition in a cellular model of multiple system atrophy, Neurochem Int, 57 (2010) 857-866.

[23] Y. Endo, T. Sawasaki, High-throughput, genome-scale protein production method based on the wheat germ cell-free expression system, J Struct Funct Genomics, 5 (2004) 45-57.

[24] S. Yurimoto, N. Hatano, M. Tsuchiya, K. Kato, T. Fujimoto, T. Masaki, R. Kobayashi, H. Tokumitsu, Identification and characterization of wolframin, the product of the wolfram syndrome gene (WFS1), as a novel calmodulin-binding protein, Biochemistry, 48 (2009) 3946-3955.

[25] F.M. Vaz, R. Ofman, K. Westinga, J.W. Back, R.J. Wanders, Molecular and Biochemical Characterization of Rat epsilon -N-Trimethyllysine Hydroxylase, the First Enzyme of Carnitine Biosynthesis, J Biol Chem, 276 (2001) 33512-33517.

[26] N. Seki, A. Hattori, S. Sugano, Y. Suzuki, A. Nakagawara, M. Muramatsu, T. Hori, T. Saito, A novel human gene whose product shares significant homology with the bovine brain-specific protein p25 on chromosome 5p15.3, J Hum Genet, 44 (1999) 121-122.

[27] M. Yamada, S. Radovick, F.E. Wondisford, Y. Nakayama, B.D. Weintraub, J.F. Wilber, Cloning and structure of human genomic DNA and hypothalamic cDNA encoding human prepro thyrotropin-releasing hormone, Mol Endocrinol, 4 (1990) 551-556.

[28] M.A. Benson, S.E. Newey, E. Martin-Rendon, R. Hawkes, D.J. Blake, Dysbindin, a novel coiled-coil-containing protein that interacts with the dystrobrevins in muscle and brain, J Biol Chem, 276 (2001) 24232-24241.

[29] J.G. Vockley, C.P. Jenkinson, H. Shukla, R.M. Kern, W.W. Grody, S.D. Cederbaum, Cloning and characterization of the human type II arginase gene, Genomics, 38 (1996) 118-123.

[30] M. Yoshihama, T. Uechi, S. Asakawa, K. Kawasaki, S. Kato, S. Higa, N. Maeda, S. Minoshima, T.

401 Tanaka, N. Shimizu, N. Kenmochi, The human ribosomal protein genes: sequencing and comparative
402 analysis of 73 genes, Genome Res, 12 (2002) 379-390.
403 [31] E. Cavdar Koc, W. Burkhart, K. Blackburn, A. Moseley, L.L. Spremulli, The small subunit of the
404 mammalian mitochondrial ribosome. Identification of the full complement of ribosomal proteins
405 present, J Biol Chem, 276 (2001) 19363-19374.
406 [32] W.J. Habets, P.T. Sillekens, M.H. Hoet, J.A. Schalken, A.J. Roebroek, J.A. Leunissen, W.J. van de
407 Ven, W.J. van Venrooij, Analysis of a cDNA clone expressing a human autoimmune antigen: full-
408 length sequence of the U2 small nuclear RNA-associated B" antigen, Proc Natl Acad Sci U S A, 84
409 (1987) 2421-2425.
410 [33] M. Raspotnig, M. Haugen, M. Thorsteinsdottir, I. Stefansson, H.B. Salvesen, A. Storstein, C.A.
411 Vedeler, Cerebellar degeneration-related proteins 2 and 2-like are present in ovarian cancer in
412 patients with and without Yo antibodies, Cancer Immunol Immunother, 66 (2017) 1463-1471.
413 [34] J.M. Williams, G.C. Chen, L. Zhu, R.F. Rest, Using the yeast two-hybrid system to identify human
414 epithelial cell proteins that bind gonococcal Opa proteins: intracellular gonococci bind pyruvate
415 kinase via their Opa proteins and require host pyruvate for growth, Mol Microbiol, 27 (1998) 171-
416 186.
417 [35] S. Sato, C. Tomomori-Sato, C.A. Banks, T.J. Parmely, I. Sorokina, C.S. Brower, R.C. Conaway, J.W.
418 Conaway, A mammalian homolog of Drosophila melanogaster transcriptional coactivator intersex is
419 a subunit of the mammalian Mediator complex, J Biol Chem, 278 (2003) 49671-49674.
420 [36] E. Hlavanda, J. Kovacs, J. Olah, F. Orosz, K.F. Medzihradszky, J. Ovadi, Brain-specific p25 protein

421 binds to tubulin and microtubules and induces aberrant microtubule assemblies at
422 substoichiometric concentrations, Biochemistry, 41 (2002) 8657-8664.
423 [37] S. DeBonis, E. Neumann, D.A. Skoufias, Self protein-protein interactions are involved in
424 TPPP/p25 mediated microtubule bundling, Sci Rep, 5 (2015) 13242.
425 [38] L. Tirian, E. Hlavanda, J. Olah, I. Horvath, F. Orosz, B. Szabo, J. Kovacs, J. Szabad, J. Ovadi,
426 TPPP/p25 promotes tubulin assemblies and blocks mitotic spindle formation, Proc Natl Acad Sci U S
427 A, 100 (2003) 13976-13981.
428 [39] G.G. Kovacs, E. Gelpi, A. Lehotzky, R. Hoftberger, A. Erdei, H. Budka, J. Ovadi, The brain-specific
429 protein TPPP/p25 in pathological protein deposits of neurodegenerative diseases, Acta Neuropathol,
430 113 (2007) 153-161.
431 [40] S. Hachem, A. Aguirre, V. Vives, A. Marks, V. Gallo, C. Legraverend, Spatial and temporal
432 expression of S100B in cells of oligodendrocyte lineage, Glia, 51 (2005) 81-97.
433 [41] J. Steiner, H.G. Bernstein, B. Bogerts, T. Gos, C. Richter-Landsberg, M.T. Wunderlich, G. Keilhoff,
434 S100B is expressed in, and released from, OLN-93 oligodendrocytes: Influence of serum and glucose
435 deprivation, Neuroscience, 154 (2008) 496-503.
436 [42] L.J. Van Eldik, J.G. Zendegui, D.R. Marshak, D.M. Watterson, Calcium-binding proteins and the
437 molecular basis of calcium action, Int Rev Cytol, 77 (1982) 1-61.
438 [43] L.J. Van Eldik, D.M. Watterson, Calmodulin and calcium signal transduction: an introduction.,
439 Academic Press, New York, 1998.
440 [44] I. Marenholz, C.W. Heizmann, G. Fritz, S100 proteins in mouse and man: from evolution to

441 function and pathology (including an update of the nomenclature), Biochem Biophys Res Commun,
442 322 (2004) 1111-1122.
443 [45] M. Takahashi, K. Tomizawa, K. Ishiguro, K. Sato, A. Omori, S. Sato, A. Shiratsuchi, T. Uchida, K.
444 Imahori, A novel brain-specific 25 kDa protein (p25) is phosphorylated by a Ser/Thr-Pro kinase (TPK
445 II) from tau protein kinase fractions, FEBS Lett, 289 (1991) 37-43.
446 [46] J. Olah, T. Szenasi, S. Szunyogh, A. Szabo, A. Lehotzky, J. Ovadi, Further evidence for microtubule-
447 independent dimerization of TPPP/p25, Sci Rep, 7 (2017) 40594.
448 [47] M.M. Fu, T.S. McAlear, H. Nguyen, J.A. Oses-Prieto, A. Valenzuela, R.D. Shi, J.J. Perrino, T.T. Huang,
449 A.L. Burlingame, S. Bechstedt, B.A. Barres, The Golgi Outpost Protein TPPP Nucleates Microtubules
450 and Is Critical for Myelination, Cell, 179 (2019) 132-146 e114.
451 [48] C. Richter-Landsberg, M. Heinrich, S-100 immunoreactivity in rat brain glial cultures is
452 associated with both astrocytes and oligodendrocytes, J Neurosci Res, 42 (1995) 657-665.
453 [49] R. Donato, Quantitative analysis of the interaction between S-100 proteins and brain tubulin,
454 Cell Calcium, 8 (1987) 283-297.
455 [50] R. Donato, Calcium-independent, pH-regulated effects of S-100 proteins on assembly-
456 disassembly of brain microtubule protein in vitro, J Biol Chem, 263 (1988) 106-110.
457 [51] R. Donato, I. Giambanco, Interaction between S-100 proteins and steady-state and taxol-
458 stabilized microtubules in vitro, J Neurochem, 52 (1989) 1010-1017.
459 [52] G. Sorci, A.L. Agneletti, R. Donato, Effects of S100A1 and S100B on microtubule stability. An in
460 vitro study using triton-cytoskeletons from astrocyte and myoblast cell lines, Neuroscience, 99

(2000) 773-783.

[53] G.G. Kovacs, L. Laszlo, J. Kovacs, P.H. Jensen, E. Lindersson, G. Botond, T. Molnar, A. Perczel, F. Hudecz, G. Mezo, A. Erdei, L. Tirian, A. Lehotzky, E. Gelpi, H. Budka, J. Ovadi, Natively unfolded tubulin polymerization promoting protein TPPP/p25 is a common marker of alpha-synucleinopathies, Neurobiol Dis, 17 (2004) 155-162.

[54] T. Szenasi, J. Olah, A. Szabo, S. Szunyogh, A. Lang, A. Perczel, A. Lehotzky, V.N. Uversky, J. Ovadi, Challenging drug target for Parkinson's disease: Pathological complex of the chameleon TPPP/p25 and alpha-synuclein proteins, Biochim Biophys Acta Mol Basis Dis, 1863 (2017) 310-323.

Acknowledgment

We thank Mami Asakura (Okayama University) for expression and purification of recombinant S100 proteins.

Figure Legends

Figure 1. Identification of S100A2-binding proteins. (A) Biotinylated S100A2 was analyzed by either SDS-PAGE, followed by CBB staining (*left panel*), or dot blotting (*right panel*) using avidin–HRP-mediated detection (1, 2, 5, and 10 ng; B, buffer). An arrow indicates biotinylated S100A2. **(B)** Biotinylated S100A2 binding of putative S100A2 targets on human protein arrays. PPI screening of recombinant human proteins using Protein Active Array®, 1,536-well format × 27 plates) containing 19,676 recombinant human proteins in duplicate was performed as described in the "**Materials and Methods 2.2.**" Array, column, and row numbers and gene symbols are indicated with each biotinylated S100A2-binding image on the array. **(C)** Putative S100A2 targets identified by PPI screening, as shown in panel B, were synthesized by the wheat germ cell-free protein synthesis as GST-fusion proteins, as described in "**Materials and Methods 2.3.,**" and were subsequently analyzed by either immunoblotting (5 µL sample) using an anti-GST antibody (*upper panel*) or an S100A2 overlay (*lower panel*). Venus protein (*Venus*) and the sample synthesized with an empty vector (*Mock*) were also included. Asterisks indicate the biotinylated S100A2-binding of synthesized target proteins. Molecular mass markers are indicated on the left side of each panel. TMLHE, trimethyllysine dioxygenase, mitochondrial isoform 1 precursor; TPPP, tubulin polymerization-promoting protein; TRH, thyrotropin-releasing hormone preproprotein; DTNBP1, dystrobrevin-binding protein 1; ARG2, arginase-2 mitochondrial precursor; RPL36, 60S ribosomal protein L36; MRPS34, mitochondrial ribosomal protein S34; SNRPB2, small nuclear ribonucleoprotein

494 polypeptide B"; CDR2L, cerebellar degeneration-related protein 2-like; OIP5, Opa interacting protein
495 5; MED29, mediator complex subunit 29.
496
497 **Figure 2. Ca^{2+}-dependent interaction of S100 proteins with TPPP *in vitro and in transfected cells*.**
498 **(A)** S100A2 (20 μg) was incubated with (+) or without (−) TPPP-His_6 (20 μg) in the presence (+) or
499 absence (−) of 2 mM $CaCl_2$ and, subsequently, pulldown with Ni-Sepharose, followed by SDS-Tricine
500 PAGE analysis (CBB staining) as described in "**Materials and Methods 2.5.**" Asterisk and arrow
501 represent TPPP-His_6 and S100A2, respectively. **(B)** COS-7 cells were transfected with expression
502 vectors encoding GST-TPPP and S100A2. After 48 h of culture, GST-TPPP was precipitated with
503 glutathione-Sepharose in the presence of 2 mM EGTA (−) or 2 mM $CaCl_2$ (+), and the precipitates
504 (*Pulldown*) were subjected to immunoblot analysis using antibodies to GST (*third panel*) and S100A2
505 (*bottom panel*) as described in "**Materials and Methods 2.6.**" The cell lysates (15 μL) from the
506 transfected COS-7 cells (*Input*) were analyzed by immunoblotting with antibodies to GST (*top panel*)
507 and S100A2 (*second panel*). Asterisks and arrows represent GST-TPPP and S100A2, respectively. **(C)**
508 S100 proteins, including S100A2, S100A4, S100A6, and S100B (40 μg), were incubated with GST-
509 TPPP-His_6 (40 μg) in the presence of 2 mM EGTA (−) or 2 mM $CaCl_2$ (+) and, subsequently, pulldown
510 with glutathione-Sepharose, followed by SDS-Tricine PAGE analysis (CBB staining). Asterisk and
511 arrow represent GST-TPPP-His_6 and S100A2, respectively.
512

Figure 3. Mapping of S100A2-binding region on TPPP. (A) Schematic representation of GST-TPPP-His_6 proteins, including full-length (residues 2–219) and mutant proteins (residues 2–174, 2–100, 101–174, and 120–174), expressed and purified in *E. coli* (*upper panel*) as described in "**Materials and Methods 2.4.**" **(B)** Purified GST-TPPP-His_6 proteins (0.2 μg), including full-length and mutant proteins, were separated on SDS-12.5% PAGE followed by the S100A2 overlay analysis (*left panel*) and immunoblot analysis using an anti-His tag antibody (*right panel*).

Figure 4. Disassembly of TPPP dimerization by Ca^{2+}/S100A2 *in vitro*. TPPP-His_6 (2.0 μg) was cross-linked with NHS/EDC with (+) or without (−) indicated amounts (0.5–1.5 μg) of S100A2 in either the absence (−) or presence (+) of 2 mM $CaCl_2$, followed by either SDS-12.5% PAGE analysis (CBB staining) **(A)** or immunoblot analysis using the anti-His tag antibody **(B),** as described in "**Materials and Methods 2.7**." Asterisks indicate the TPPP-His_6 monomer cross-linked with S100A2. A left lane (*N*) in **B** indicates TPPP-His_6 sample without NHS/EDC treatment. **(C)** Proposed model for regulation of TPPP dimerization by Ca^{2+}/S100 protein.

Figure 5. Ca^{2+}-dependent disassembly of TPPP dimerization by S100A6 and S100B *in vitro*. TPPP-His_6 (2 μg) was cross-linked with NHS/EDC with (+) or without (−) indicated amounts (0.5 and 1.0 μg) of S100A4 **(A)**, S100A6 **(B)**, or S100B **(C)** in either the absence (−) or presence (+) of 2 mM $CaCl_2$, followed by immunoblot analysis using the anti-His tag antibody, as described in "**Materials and**

532 **Methods 2.7**." A right lane (*N*) in each panel indicates the TPPP-His_6 sample without NHS/EDC

533 treatment. Asterisks indicate the TPPP-His_6 monomer cross-linked with the S100 proteins.

534

Doi *et al*. Figure 1

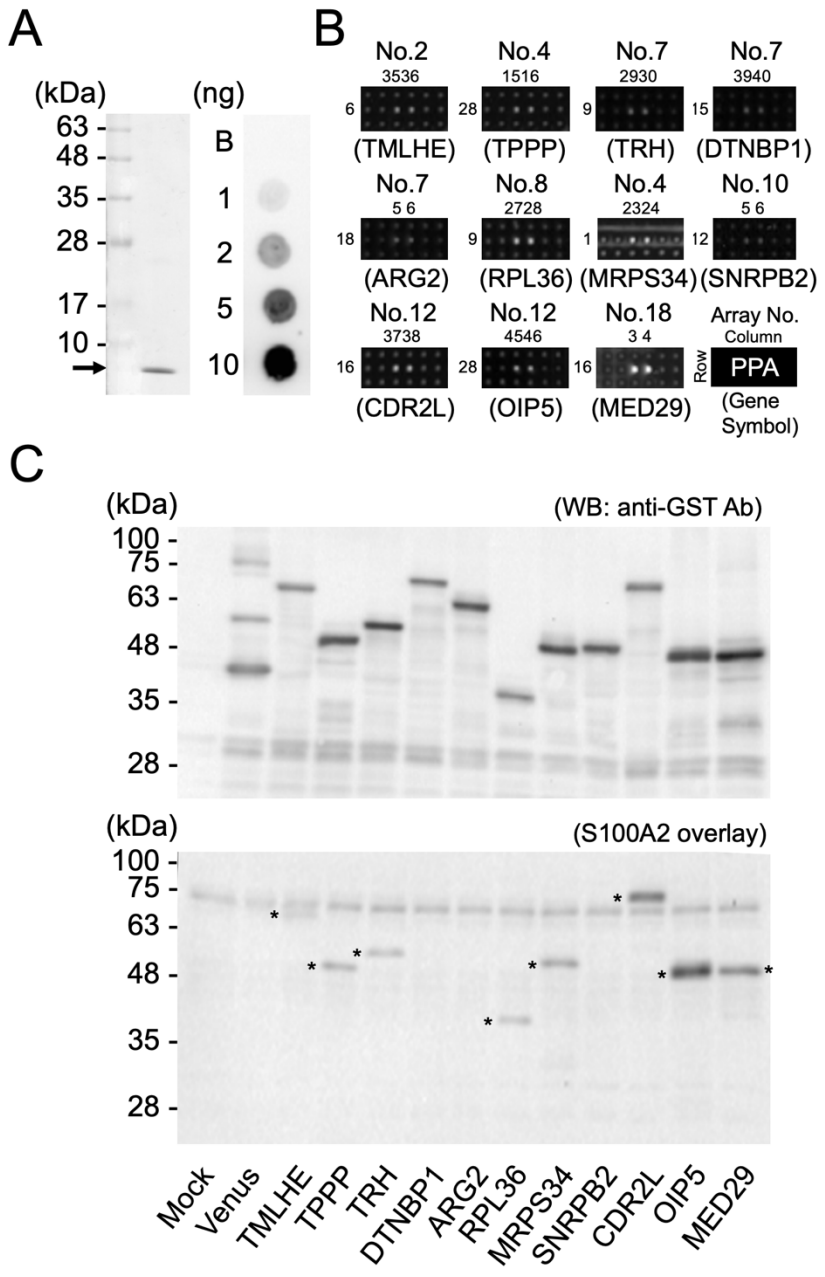

535

536

Doi *et al*. Figure 2

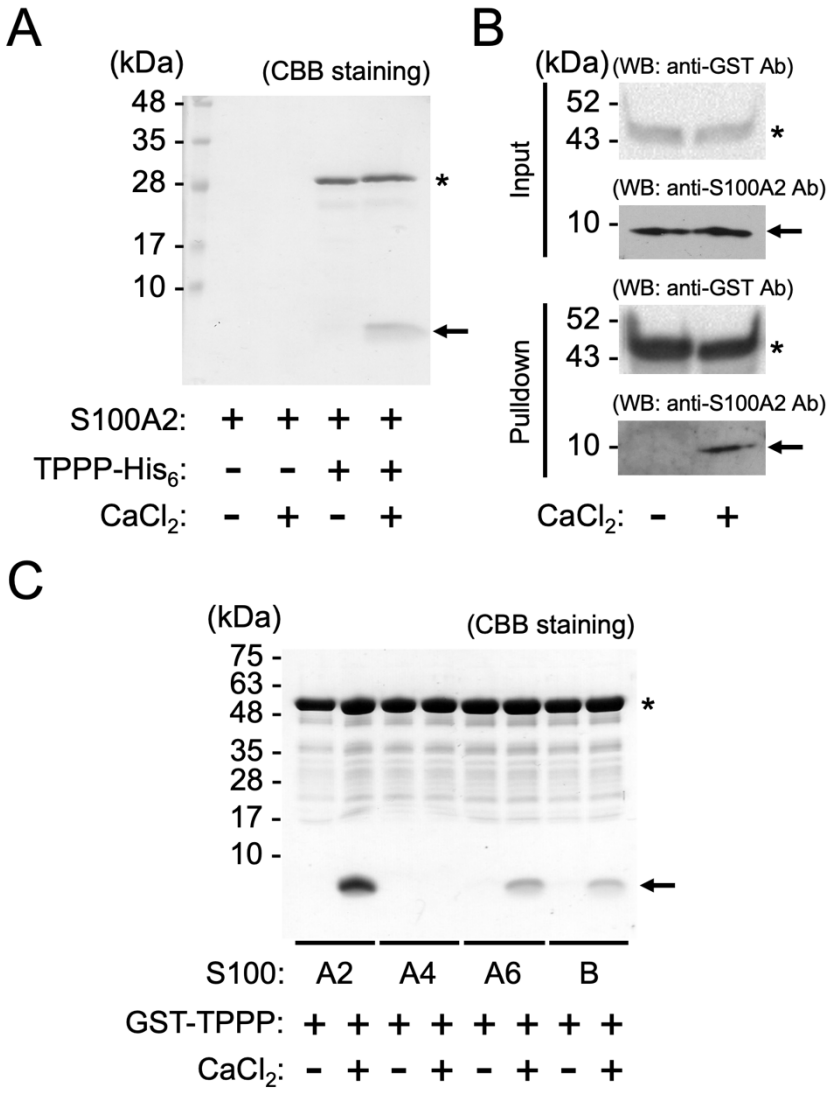

537

Doi *et al*. Figure 3

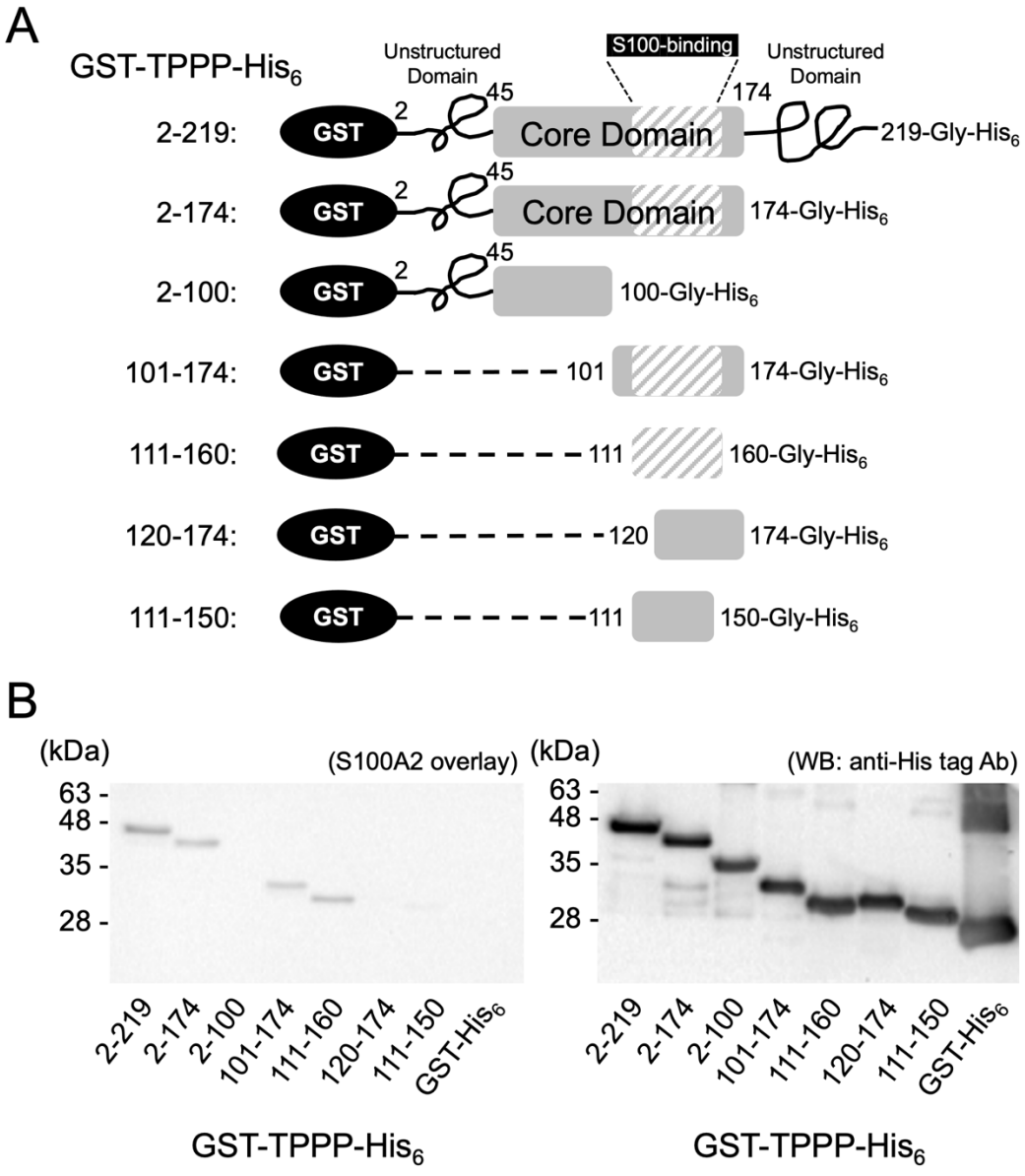

538

539

Doi *et al*. Figure 4

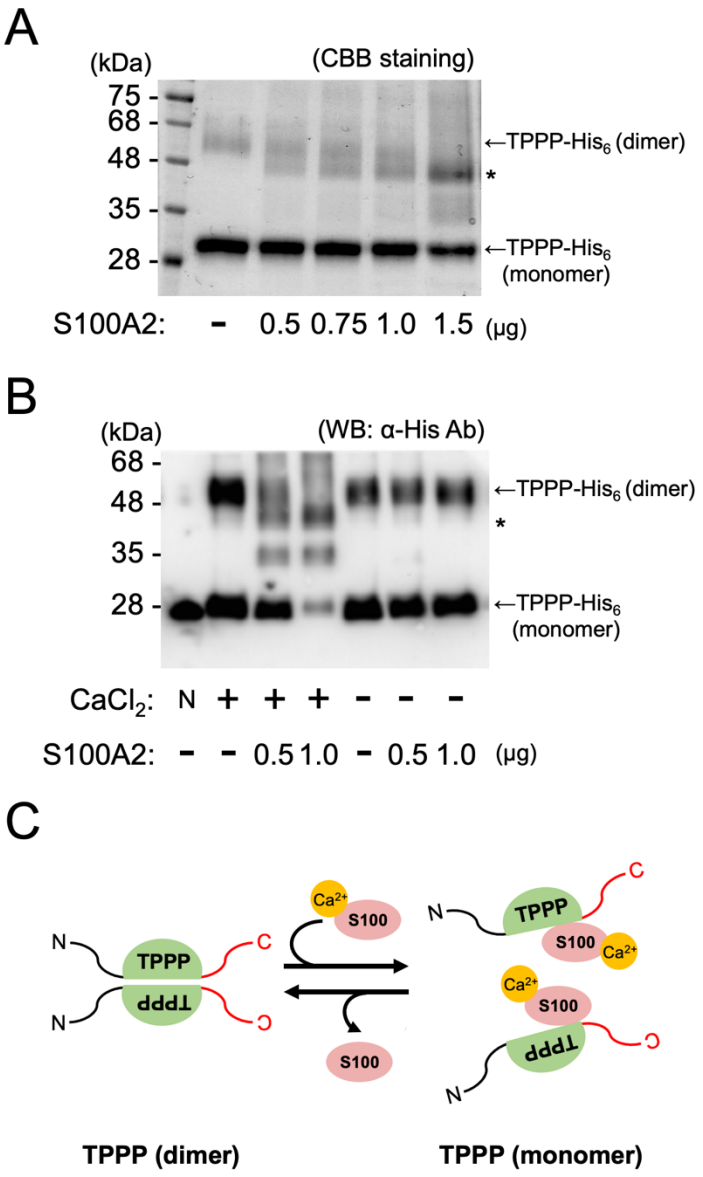

540

541

Doi *et al*. Figure 5

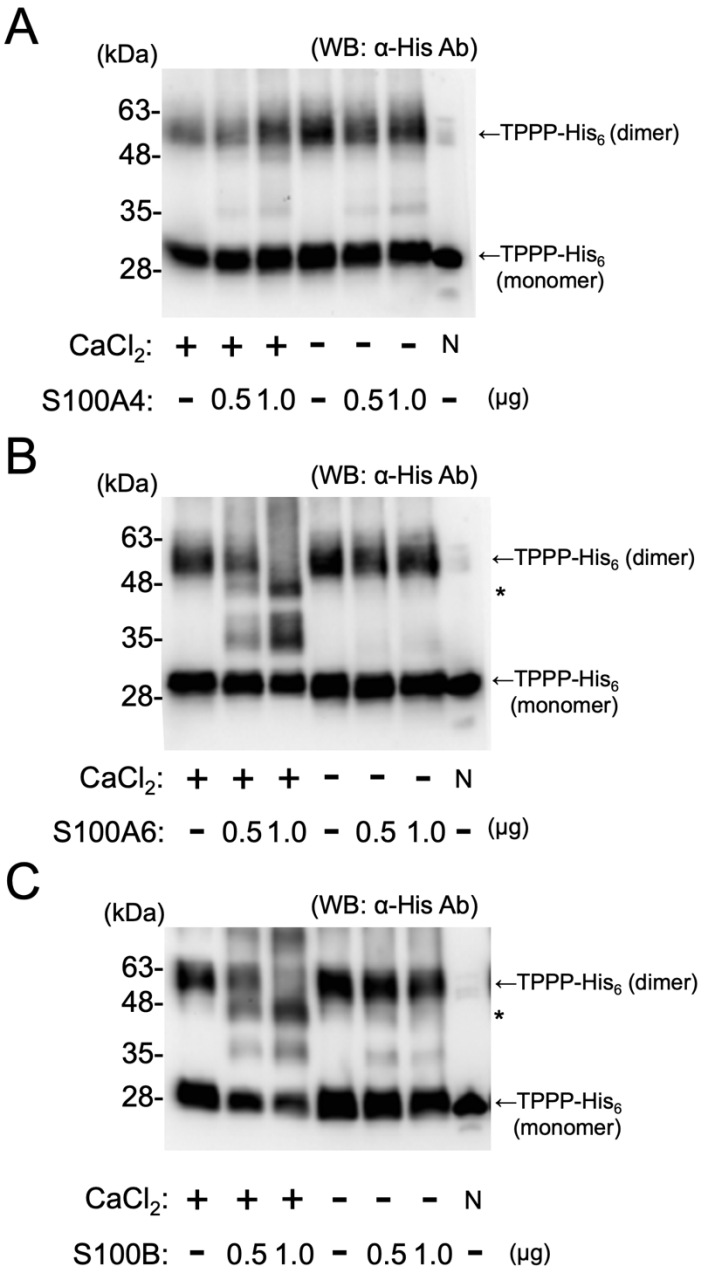

542

543

Supplemental Figure S1

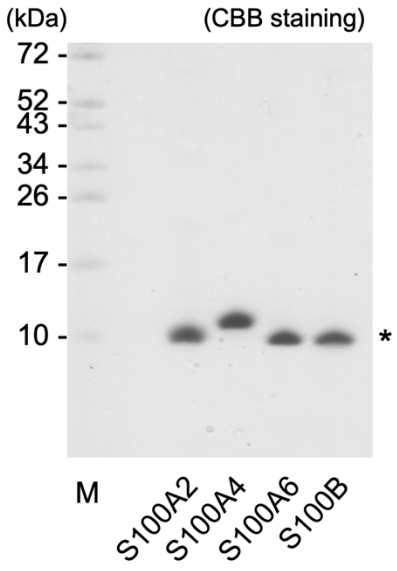

Supplemental Figure S1. Recombinant S100A2, S100A4, S100A6 and S100B (1 μg) were subjected to SDS-Tricine PAGE, followed by Coomassie Brilliant Blue (CBB) staining. An asterisk indicates S100 protein. M indicates molecular mass markers.

Supplemental Figure S2

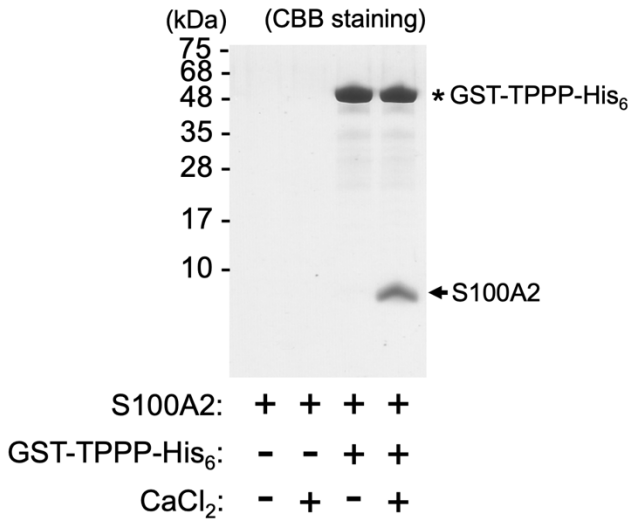

Supplemental Figure S2. S100A2 was incubated with (+) or without (-) GST-TPPP-His_6 in the presence of 2 mM EGTA (−) or 2 mM $CaCl_2$ (+) and, subsequently, pulldown with glutathione-Sepharose, followed by SDS-Tricine PAGE analysis (CBB staining). An asterisk and an arrow indicate GST-TPPP-His_6 and S100A2, respectively.

546

547